Proceedings of the ASME 2010 3rd Joint US-European Fluids Engineering Summer Meeting and 8th International Conference on Nanochannels, Microchannels, and Minichannels
FEDSM-ICNMM2010
August 1-5, 2010, Montreal, Canada

FEDSM-ICNMM2010-30637

AN EXPERIMENTAL STUDY OF THE NEAR-WAKE STRUCTURE OF A CYLINDER UNDERGOING COMBINED TRANSLATIONAL AND ROTATIONAL OSCILLATORY MOTIONS

Mehdi Nazarinia
Mark C. Thompson
John Sheridan*
Fluids Laboratory for Aeronautical and
Industrial Research (FLAIR)
Department of Mechanical and Aerospace Engineering
Monash University
P.O. Box 31, Melbourne, Victoria 3800
Email: mehdi.nazarinia@eng.monash.edu.au
mark.thompson@eng.monash.edu.au
john.sheridan@eng.monash.edu.au

David Lo Jacono
Université de Toulouse; INPT, UPS;
IMFT (Institut de Mécanique des Fluides de Toulouse);
Allée Camille Soula, F-31400
Toulouse, France
CNRS; IMFT; F-31400 Toulouse, France
FLAIR, Department of Mechanical and Aerospace Engineering
Monash University
P.O. Box 31, Melbourne, Victoria 3800
Australia
Email: david.lojacono@imft.fr

ABSTRACT

The experimental research reported here uses particle image velocimetry to extend the study of Nazarinia et al. [1], recording detailed vorticity fields in the near-wake of a circular cylinder undergoing combined translational and rotational oscillatory motions. The focus of the present study is to examine the effect of the ratio between the translational and rotational velocities of the cylinder on the synchronization of the near-wake structures. The frequencies are fixed close to that of the natural frequency of vortex shedding. The results are presented for a fixed amplitude of rotational oscillation of 1 radian and a range of ratios between the translational and rotational velocities (V_R) $= [0.25, 0.5, 1.0, 1.5]$. In particular, it was found that varying the V_R value changed the near-wake structure. The results show that at lower values of $V_R = 0.25$, for all of the phase differences examined, the vortices are shed in a single-row $2S$ mode aligned in the medial plane with a slight offset from the centerline and also synchronized with the combined oscillatory motion. As V_R increases the vortex shedding mode changes from a $2S$ single-row to a $2S$ double-row structure and eventually back to the single-row (at $V_R = 0.5$). Increasing V_R further resulted in the appearance of unlocked-on regimes over the range of negative phase angles and a transition from $2S$ to $P+S$ mode at the in-phase case There was transition back to the $2S$ with a further decrease of Φ. For a higher V_R the range of desynchronization increased.

NOMENCLATURE

θ Angular displacement
β Stokes number
μ Dynamic viscosity (kg.m^{-1}.s^{-1})
ν Kinematic viscosity, μ/ρ, (m^2.s^{-1})
ω_x, ω_y, ω_z Vorticity components along the x, y and z axis respectively (s^{-1})
Φ Phase angle between rotational and translational motions
A_θ Amplitude of rotational oscillation in radians
A_t Amplitude of translational oscillation
D Cylinder diameter
f frequency of oscillation (Hz)
f_N Natural frequency of vortex shedding (Hz)

*Address all correspondence to this author.

f_v Frequency of vortex shedding (Hz)
F_R Frequency ratio between translational and rotational oscillation = f_t/f_θ
F_{RN} Frequency ratio between oscillatory motion and natural frequency = f/f_N
F_{Rt} Frequency ratio between translational oscillation and natural frequency = f_t/f_N
$F_{R\theta}$ Frequency ratio between rotational oscillation and natural frequency = f_θ/f_N
KC Keulegan-Carpenter number
PIV Particle image velocimetry
Re Reynolds number based on free-stream velocity and cylinder diameter= $(U_\infty D)/\nu$
St Strouhal number
$U_{\max}$ Peak velocity of an oscillating cylinder
U_∞ Free-stream velocity
V_R Velocity ratio between translational and rotational oscillation = $U_{\max_t}/U_{\max_\theta}$
y Translational displacement

INTRODUCTION

Studies on flow past an oscillating cylinder can be divided into three categories depending on the motion of the cylinder: the cylinder oscillates translationally only at an angle with respect to the free-stream; the cylinder performs a rotational oscillation about its axis in mean flow; the flow is created by a circular cylinder moving with combined oscillatory translational *and* rotational motion in quiescent fluid or free-stream. Many researchers (such as [2–12] and many more) have shown that the vortex shedding phenomenon can be dramatically altered for the cylinder undergoing either in-line or transverse oscillation in a fluid stream. There has also been considerable research on the purely rotational oscillation case (see for example: [13–18]). The latter is a class of flow that has not received as much attention as the case of purely oscillating cylinders have, until now. Blackburn *et al.* [19] found that a circular cylinder undergoing combined oscillation in a quiescent fluid has the capability to generate thrust, *i.e. "swimming cylinder"*. Nazarinia *et al.* [1, 20] extended their study and for the first time experimentally measured the flow around a circular cylinder undergoing combined translational and rotational oscillation in a free-stream and quiescent fluid, respectively. Placing the circular cylinder which is undergoing combined oscillatory motion in a free-stream has been shown to generate intriguing wake modes and has also been found to have the potential to reduce synchronization of the cylinder motion in the near-wake [1, 21, 22]. Nazarinia *et al.* [1] experimentally and numerically studied the flow behind a cylinder undergoing forced combined oscillatory motion. The focus of this paper was on the effect of the Φ angle between the two motions but the influence of the velocity ratio between them was not considered. They found that there is an unexpected loss of synchronization of the wake for a finite range of phase differences. The primary focus of the reported study here is to understand and investigate the effect of V_R on the synchronization of the cylinder motion in the near-wake. Improving our understanding of how to effect desynchronization increases the likelihood that such approaches can be used in the active or passive control of vortex-induced vibration.

PROBLEM DEFINITION

The equations of the forcing motions, consisting of two independent oscillations: cross-stream translation and rotation, are:

$$y(t) = A_t \sin(2\pi f_t t), \quad (1)$$
$$\theta(t) = A_\theta \sin(2\pi f_\theta t + \Phi). \quad (2)$$

The flow past a cylinder undergoing combined translation and rotation oscillations depends on the six independent parameters defined by Eqns. (3)–(5) and the phase difference between the motions (Φ), as defined by Eqn. (2). The dimensionless quantities representative of independent variables are defined as follows:

$$KC_t = \frac{U_{\max_t}}{f_t D} = \frac{2\pi A_t}{D}, \qquad KC_\theta = \frac{U_{\max_\theta}}{f_\theta D} = \pi A_\theta, \quad (3)$$
$$F_{Rt} = \frac{f_t}{f_N}, \qquad F_{R\theta} = \frac{f_\theta}{f_N}, \quad (4)$$
$$Re = \frac{U_\infty D}{\nu}. \quad (5)$$

The cylinder's velocity ratio, between the translational and rotational motions can also be expressed as:

$$V_R = \frac{U_{\max_t}}{U_{\max_\theta}}. \quad (6)$$

Figure 1 shows a schematic of the problem studied with some relevant notations and features. The Cartesian coordinate system in use is defined such that the origin is located at the center of the circular cylinder (at $t = 0$) with x, y and z representing the streamwise, transverse, and spanwise directions, respectively.

METHODS AND TECHNIQUES

Experimental Setup

The experiments were conducted in the FLAIR free-surface closed-loop water channel at the Department of Mechanical and

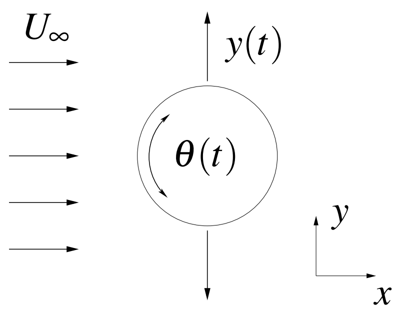

FIGURE 1. Schematic showing the problem geometry and important parameters relevant to the combined forced oscillation and the circular cylinder model. The streamwise direction is the x-direction.

Aerospace Engineering, Monash University. Detailed information of the set-up can be found in [1, 20]. The cylinder used was 800mm in length with an outer diameter of 20mm, giving an aspect ratio of 40. The experiments were performed for a fixed average upstream velocity $U_\infty = 0.0606$m/s giving $Re_{avg} = 1\,322$. The frequencies of the motions are fixed close to that of the natural frequency ($T^{-1} = f_t = f_\theta = 0.6\text{s}^{-1} \approx f_N$). The natural frequency was found to be equal to $f_N \approx 0.6154\text{s}^{-1}$. The Strouhal number based on this frequency is about $St \approx f_N D/U_\infty = 0.203$ and the Strouhal number of the forcing is $St_t \approx f_t D/U_\infty = 0.198$. The results of experiments presented here are for (a) a fixed amplitude of rotational oscillation of 1 radian and a range of $0.25 \le V_R \le 1.5$ and (b) Case 5 has a reduced amplitude of rotational oscillation of 0.5 radians and $V_R = 1$. For each V_R case the phase difference angle was varied during measurements. Table 1 summarizes the data points measured in the present study.

The cylinder was oscillated translationally and rotationally by using two high-resolution stepper motors. The translational stepper motor actuated the rodless in-line mounting actuator and the rotational stepper motor was connected directly to the vertically mounted cylinder. The stepper motors were controlled using a two-axis indexer and two high-resolution drivers (running at 50800 steps rev^{-1}). A pure sinusoidal profile, as defined in Eqns. 1 and 2, is used throughout the paper. A TTL-signal triggered other devices (camera and laser), thus images could be captured at pre-selected phase angles in the oscillation cycle (phase-locked).

Experimental Techniques

The method used here to characterize the wake of this forced cylinder is via PIV. The PIV set-up was based on that originally described by Adrian [23] and developed in-house over the past decade [24]. The flow was seeded with spherical granular polyamide particles having a mean diameter of 55μm and specific gravity of 1.016. The particles were illuminated using two mini-YAG laser sources (Continuum Minilite II Q-Switched).

TABLE 1. SUMMARY OF THE VALUES OF A_t AND A_θ USED WHEN F_R=1.0.

Case	A_t	A_θ(rad)	V_R	$U_{\max_t}$(ms^{-1})	$U_{\max_t}/U_\infty$
1	$D/8$	1.0	0.25	0.0094	0.16
2	$D/4$	1.0	0.5	0.0188	0.31
3	$D/2$	1.0	1.0	0.0377	0.62
4	$3D/4$	1.0	1.5	0.0565	0.93
5	$D/4$	0.5	1.0	0.0188	0.31

The plane of interest for these experiments was orthogonal to the cylinder's axis (xy-plane) and downstream (x-direction) of the cylinder. A small section of the cylinder is replaced by a thin-walled transparent cylinder, whose interior is filled with distilled water. It is located at about 9D from the end of cylinder. The measured xy-plane is located through the centre of this window. The thickness of the laser sheet was measured to be approximately less than 2mm. Pairs of images were captured on a high resolution CCD camera with a maximum resolution of 4008×2672 pixels. The camera was equipped with a 105mm lens (Nikon Corporation, Japan). At a particular phase of the oscillation cycle, a number of image pairs over successive cycles were taken and stored for further processing. The timing of the laser and camera triggering was controlled by a special in-house designed timing unit, with an estimated accuracy of 1μs.

Each image pair was processed using in-house PIV software [24]. This software uses a double-frame, cross-correlation multi-window algorithm to extract a grid of displacement vectors from the PIV images. An interrogation window of 32×32 (with an initial window size of 64×64) pixels was found to give satisfactory results with 50% overlap. More than 98% of the vectors were found to be valid for all the experiments. It was possible to obtain a measurement resolution of 127×127 vectors in each field of view. The overall field of view was 4008×2672 pixels ($6.0D \times 6.0D$).

Our PIV set-up and technique have been validated against the previous numerical and experimental results [25, 26] for the xy- and yz-plane measurements. The validation case studied is for a purely translational oscillation in a quiescent fluid. Further information can be found in [20].

RESULTS AND DISCUSSION

In this section the results are presented for velocity ratios of 0.25, 0.5, 1.0 and 1.5. The wake profiles around the cylinder in the streamwise direction xy-plane for F_R=1.0 and $Re_{avg} = 1,322$ are investigated. Due to the change in the temperature of the water the actual Re number of each set of experiments might be marginally different from the averaged value, which is presented for each set of experiments in the relevant figure. It should also be noted that the field-of-view does not allow us to see the flow structures that occur farther downstream, however the near-wake flow structures are the main focus of this study. For every value of V_R studied, the effect of a change of phase difference angle on the synchronization of the near-wake has also been examined. However, in this paper only selected phases are discussed and presented.

Figure 2 presents the near-wake motion phased-locked vorticity and root-mean-square (rms) vorticity contours taken at $t = T$ for various V_R values at $\Phi = 0°$ i.e. in-phase. The image at the top left of Fig. 2 shows the case where the velocity ratio is 0.25. In this case we observe a $2S$ mode (2 single vortices of opposite sign shed per period) in a single-row aligned in the medial plane but with a slight offset from the centreline. The field-of-view does not allow us to see the double-row that should occur further downstream (see for example [27–29]). The classification of the different vortex modes is given by [9]. Throughout the observations it can be seen that the near-wake vortices remain coherent in the near-wake and are synchronized with the translational motion, at least up to $6D$ downstream. This synchronization is characterized by the repeatable pattern of the vortex shedding. Examination of the U/U_∞ and V/U_∞ velocity contours, not shown here, also suggests that the velocity structures are not changed significantly by changing the phase difference angle and that the vortices are synchronized with the translational motion, *i.e.* locked. Note that setting the V_R to such a small value means the rotational oscillatory speed is much faster than the translational. This locking-on can be explained by the rotational oscillation adding momentum to the flow.

Figure 2b shows the phased-locked vorticity and rms vorticity contours for V_R=0.5. In this case the vortices are still shed in a $2S$ single-row mode and are coherent. However,the vortices are arranged closer to each other and are less well-aligned with the medial plane, suggesting an earlier double-row transition. The rms vorticity, image (b) of Fig. 2, along with U/U_∞ and V/U_∞ velocity contours not shown here, have a similar trend and configuration to the previously discussed case, confirming that the near-wake still synchronizes with the combined motion. However, a change in the phase difference between the two motions results in a change of shedding mode from a single-row to double-row.

Increasing the V_R further to 1.0, image (c) of Fig. 2, changes the vortex shedding mode to the signature of a $P+S$ mode (a single vortex and a vortex pair formed per cycle) in the near-wake, in comparison with the $2S$ mode observed in the previous cases. For this case, the vortices are shed widely apart (nearly $4D$), which is readily explained by the rotational oscillation adding momentum to the translational motion. The resulting strain favours a transition to the $P+S$ wake [30].

Figure 2d shows the phased-locked vorticity and rms vorticity contours for V_R=1.5. The shedding mode for this case is $P+S$. The vortices are more defined in the vortex street and are observed to be synchronized with the motions. The vortices are more widely aligned than those seen in image (c).

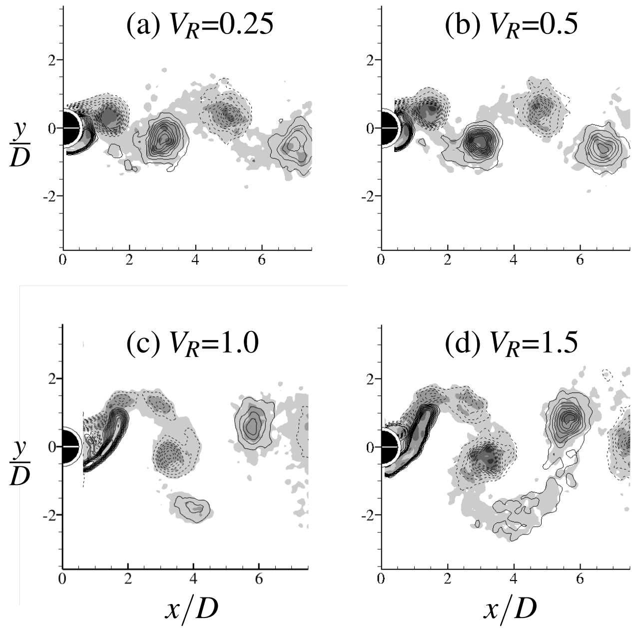

FIGURE 2. Motion phased-locked vorticity contours (lines) and root-mean-square vorticity (gray-scale) contours taken at the motion-phase of $t = T$ for $A_\theta = 1.0$, $\Phi = 0°$, f_N=0.6 Hz, F_R=1 and $Re_{avg} = 1322$. The near-wake vorticity is shown for different V_R values. The flow direction is from left to right. Root-mean-square vorticity contours are evenly spaced over the range $[0.02 : 0.1]$; with $\Delta\omega_z = 0.02$, and vorticity contours are evenly spaced over the range $[-0.1 : 0.1]$; with $\Delta\omega_z rms = 0.01$.

In the results presented to this point the change of V_R was investigated by varying A_t and keeping $A_\theta = 1$ radian. In Fig. 3 A_θ was reduced to 0.5 radians while V_R was set to 1.0. This allows us to directly compare the vorticity patterns with those of image (c) of Fig. 2, which has the same V_R but A_θ=1 radian. It can be observed that the vortices in Fig. 3 are all larger in size than those shown in Fig. 2 and are well-formed. The near-wakes for all of the Φ values are synchronized with the motions and the shedding mode is $2S$. It can be seen that even though the $V_R = 1.0$ is the same for the two cases 3 and 5 of Table 1 the near-wake structure is completely different. No transition between shedding modes can be observed as Φ is varied. In case 3, because the rotational amplitude is greater than that of case 5, it adds momentum more compactly into the flow, hence the vortices are more compact and the phase difference does not influence the synchronization of the near-wake nor the vortex shedding mode. Root-mean-square vorticity and velocity contours all confirm the synchronization of the near-wake. The velocity patterns are qualitatively similar to

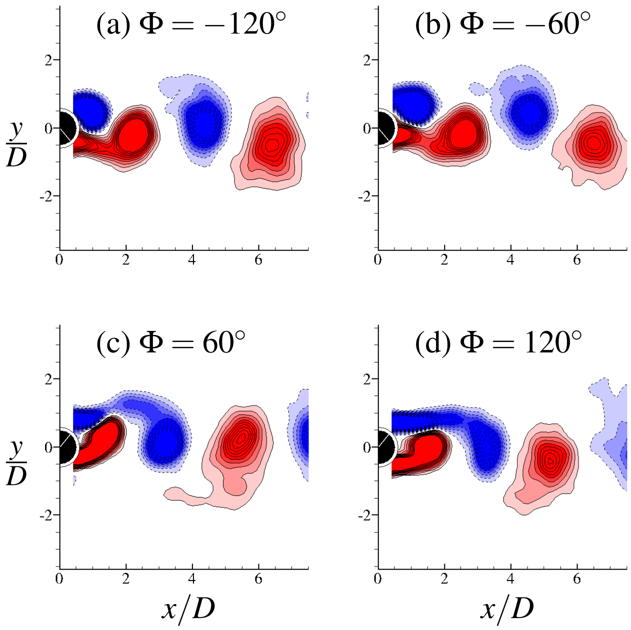

FIGURE 3. Motion phased-locked vorticity contours taken at the motion-phase of $t = T$ for f_N=0.6 Hz, F_R=1, $A_t = D/4$, $A_\theta = 0.5$ radian and $Re_{avg} = 1\,322$. The near-wake vorticity is shown for different Φ values. The flow direction is from left to right. Vorticity contours are evenly spaced over the range $[-0.1 : 0.1]$; with $\Delta\omega_z rms = 0.01$.

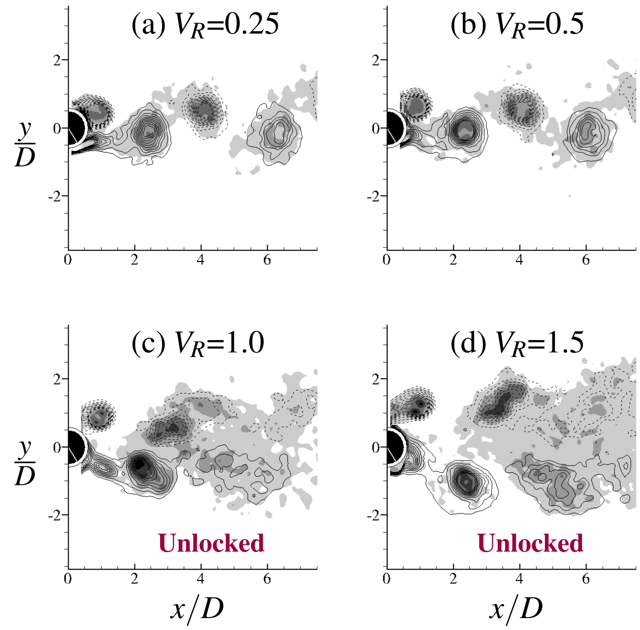

FIGURE 4. Motion phased-locked vorticity contours (lines) and root-mean-square vorticity (gray-scale) contours taken at the motion-phase of $t = T$ for $A_\theta = 1.0$, $\Phi = -90°$, f_N=0.6 Hz, F_R=1 and $Re_{avg} = 1\,322$. The near-wake vorticity is shown for different V_R values. Of particular interest is the unlocked (asynchronous) wake with the imposed translational motion for the velocity ratios of 1.0 and 1.5. The flow direction is from left to right. Root-mean-square vorticity contours are evenly spaced over the range $[0.02 : 0.1]$; with $\Delta\omega_z = 0.02$, and vorticity contours are evenly spaced over the range $[-0.1 : 0.1]$; with $\Delta\omega_z rms = 0.01$.

the locked previous cases and no evidence of transition between states can be observed.

Figures 4 and 5 present the near-wake motion phased-locked vorticity and rms vorticity contours and V/U_∞ velocity contours, respectively, taken at $t = T$ for various V_R values at A_θ and $\Phi = -90°$. The near-wake vortex structures and vortex modes of images (a) and (b) in Fig. 4 are similar to those of Fig. 2. The vortices are not separated widely and remain less than $1D$ from the centreline. The $2S$ mode in a single-row aligned in the medial plane with a slight offset from the centreline was observed. Increasing the V_R value at the same Φ was found to change the synchronization effect dramatically as can be seen in Fig. 4c and d. The rms vorticity contours clearly show how the near-wake has changed its structure. Contrary to the other cases shown in images (a) and (b), these two cases were not synchronized with the motions beyond $2D$ downstream. The effect of this loss of synchronization can be seen in the rapid downstream dissipation of the mean vortex structures. Only the two vortices near the cylinder remain coherent. This *a priori* surprising phenomenon might be explained by the fact that the separation between the two rows of vortices is smaller and that this arrangement of vortices is not stable. Similar behaviour has been found behind elliptical cylinders [29].

Comparing the V/U_∞ and rms vorticity contours of this case (Fig. 5 and 4) with the previous cases shows that there is a dramatic change of patterns in the velocity contours between the synchronized and desynchronized cases. The synchronized velocity patterns are all well organised and qualitatively similar to each other. Figure 5 clearly shows that the V velocity contour pattern has changed dramatically for the unlocked cases and for distances farther downstream beyond approximately $3D$ the dissipation of vortices is more apparent.

For the $V_R = 1$ case shown in FIg. 4 the contours of vorticity that have been phase-averaged with the cylinder's motion appear to coincide with those of the rms vorticity patterns, despite the wake being unlocked for this case. Similar trends were also found to apply in the cases of which is not shown here is applicable to the $\Phi = \pm 180°, -120°$ and $-150°$. They are not well formed and the structures of the vortices are not coherent. This pattern shows that the flow is not synchronized and the perturbations are clearly visible in those regions, hence they are all unlocked.

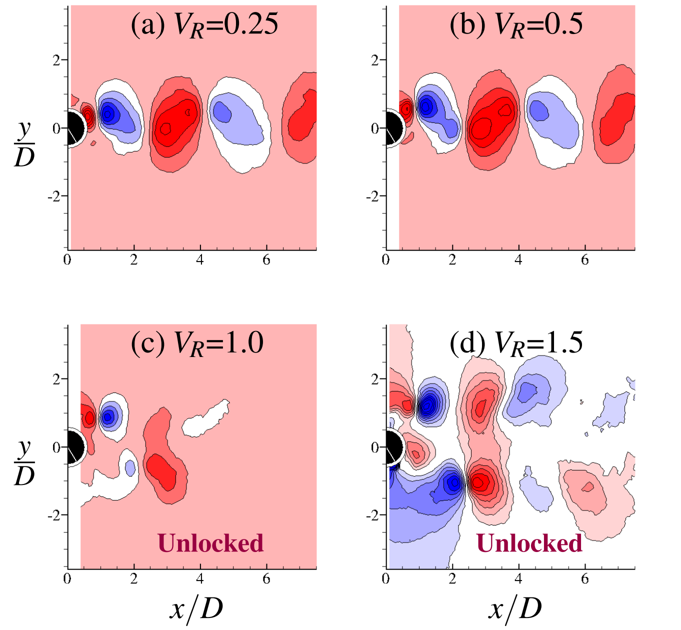

FIGURE 5. Motion phased-locked V/U_∞ velocity contours taken at the motion-phase of $t = T$ for $A_\theta = 1.0$, $\Phi = -90°$, f_N=0.6 Hz, F_R=1 and $Re_{avg} = 1322$. The velocity contours are shown for different V_R values. Of particular interest is the unlocked (asynchronous) wake with the imposed translational motion for the velocity ratios of 1.0 and 1.5. The flow direction is from left to right. V/U_∞ velocity contours are evenly spaced over the range $[-0.2 : 2.4]$; with $\Delta(V/U_\infty) = 0.2$.

CONCLUSIONS

In this work we have experimentally investigated the near-wake flow structures of flow past a cylinder undergoing a combined translation and rotation oscillatory motion. The effect of the velocity ratio between the two forced motions for a given Reynolds number and combination of Φ reveals that regular vortex shedding can be suppressed for particular phase differences and V_R values. The range of phase difference for which the suppression occurs depends on the V_R and F_R of the oscillations and the oscillation frequency ratio to natural vortex shedding frequency of a fixed cylinder. At the lower values of V_R, over the range of phase difference angles studied, no transition to different wake modes is observed. All the vortices in the near-wake region of the cylinder are synchronized and coherently shed in the $2S$ mode. Increasing the V_R value beyond a certain value changes the wake modes and the synchronisation of the vortices in the near-wake. The vortices become unlocked and less coherent as V_R is increased further for a range of Φ. The effect of changing translational and rotational amplitudes for a given V_R, *i.e.* V_R=1.0, was also investigated. It appears that at higher A_t and lower A_θ the vortices in the near-wake are more compact and larger in size. Changing the A_t and A_θ did not, however, seem to have an effect on the synchronisation of the vortices and the wake shedding modes. This experimental study raised several interesting features which determine the wake modes in the near-wake of the combined oscillatory cylinder in free-stream. One particularly interesting question is whether the desynchronized state has a chaotic or quasi-periodic form. This will require further investigation using higher frequency sampling than is possible with the current PIV system. The answer is likely to be revealed by a combination of Laser Doppler Anemometer experiments and numerical modeling.

ACKNOWLEDGMENT

M.N. would like to acknowledge the support of a Monash Graduate Scholarship (MGS) and Monash International Postgraduate Research Scholarship (MIPRS). We also acknowledge support from ARC Discovery Grant No. DP0774525 and the Australian Partnership for Advanced Computing (APAC).

REFERENCES

[1] Nazarinia, M., Lo Jacono, D., Thompson, M. C., and Sheridan, J., 2009. "Flow behind a cylinder forced by a combination of oscillatory translational and rotational motions". *Phys. Fluids,* ***21***(5), p. 051701.

[2] Bishop, R. E. D., and Hassan, A. Y., 1964. "The lift and drag forces on a circular cylinder oscillating in a flowing fluid.". *Proceedings of the Royal Society of London, series A,* ***277***(1368), pp. 51–75.

[3] Koopmann, G. H., 1967. "The vortex wakes of vibrating cylinders at low Reynolds numbers.". *J. Fluid Mech.,* ***28***, pp. 501–512.

[4] Bearman, P. W., and Currie, I. G., 1979. "Pressure fluctuation measurements on an oscillating circular cylinder". *J. Fluid Mech.,* ***91***, pp. 661–677.

[5] Sarpkaya, T., and Isaacson, M., 1981. *Mechanics of Wave Forces on Offshore Structures*. Van Nostrand Reinhold Company.

[6] Bearman, P. W., Graham, J. M. R., Naylor, P., and Obasaju, E. D., 1981. "The role of vortices in oscillatory flow about bluff cylinders". In International Symposium on Hydrodynamics in Ocean Engineering, pp. 621–635.

[7] Bearman, P. W., 1984. "Vortex shedding from oscillating bluff bodies". *Annu. Rev. Fluid Mech.,* ***16***(1), pp. 195–222.

[8] Williamson, C. H. K., 1985. "Sinusoidal flow relative to circular cylinders". *J. Fluid Mech.,* ***155***, pp. 141–174.

[9] Williamson, C. H. K., and Roshko, A., 1988. "Vortex formation in the wake of an oscillating cylinder". *J. Fluid. Struct.,* ***2***(4), pp. 355–381.

[10] Carberry, J., Sheridan, J., and Rockwell, D., 2001. "Force and wake modes of an oscillating cylinder". *J. Fluid. Struct.,* ***15***, pp. 523–532.

[11] Uzunoğlu, B., Tan, M., and Price, W. G., 2001. "Low-Reynolds-number flow around an oscillating cylinder using a cell viscous boundary element method". *Int. J. Numer. Meth. Engng.,* ***50***, pp. 2317–2338.

[12] Leontini, J. S., Stewart, B. E., Thompson, M. C., and Hourigan, K., 2006. "Predicting vortex-induced vibration from driven oscillation results". *Appl. Math. Model.,* ***30***, pp. 1096–1102.

[13] Wu, J. M., Mo, J. D., and Vakili, A. D., 1989. "On the wake of a cylinder with rotational oscillations". In AIAA 2nd Shear Flow Conference, AIAA-89-1024, pp. 1–10.

[14] Tokumaru, P. T., and Dimotakis, P. E., 1991. "Rotary oscillation control of a cylinder wake". *J. Fluid Mech.,* ***224***, pp. 77–90.

[15] Filler, J. R., Marston, P. L., and Mih, W. C., 1991. "Response of the shear layers separating from a circular cylinder to small amplitude rotational oscillations". *J. Fluid Mech.,* ***231***, pp. 481–499.

[16] Schmidt, C. W., and Smith, D. R., 2004. "An investigation of the wake behind a circular cylinder with sinusoidal rotational forcing". In 42nd AIAA Aerospace science meeting & exhibit, Reno, NV, USA, AIAA-2004-0924, pp. 1–9.

[17] Thiria, B., Goujon-Durand, S., and Wesfreid, J. E., 2006. "The wake of a cylinder performing rotary oscillations". *J. Fluid Mech.,* ***560***, pp. 123–147.

[18] Lo Jacono, D., Leontini, J. S., Thompson, M. C., and Sheridan, J., 2010. "Modification of three-dimensional transition in the wake of a rotationally oscillating cylinder". *J. Fluid Mech.,* ***643***, pp. 349–362.

[19] Blackburn, H. M., Elston, J. R., and Sheridan, J., 1999. "Bluff-body propulsion produced by combined rotary and translational oscillation". *Phys. Fluids,* ***11***(1), pp. 4–6.

[20] Nazarinia, M., Lo Jacono, D., Thompson, M. C., and Sheridan, J., 2009. "The three-dimensional wake of a cylinder undergoing a combination of translational and rotational oscillation in a quiescent fluid". *Phys. Fluids,* ***21***(6), p. 064101.

[21] Al-Mdallal, Q. M., 2004. "Analysis and computation of the cross-flow past an oscillating cylinder with two degrees of freedom". PhD thesis, Memorial University of Newfoundland.

[22] Kocabiyik, S., and Al-Mdallal, Q. M., 2005. *Bluff-body flow created by combined rotary and translational oscillation*, Vol. 84 of *Fluid Structure Interaction and Moving Boundary Problems*. WIT Press, Southampton, UK, pp. 195–203.

[23] Adrian, R. J., 1991. "Particle-imaging techniques for experimental fluid mechanics". *Annu. Rev. Fluid Mech.,* ***23***, pp. 261–304.

[24] Fouras, A., Lo Jacono, D., and Hourigan, K., 2008. "Target-free stereo PIV: A novel technique with inherent error estimation and improved accuracy". *Exp. Fluids,* ***44***(2), pp. 317–329.

[25] Dütsch, H., Dusrt, F., Becker, S., and Lienhart, H., 1998. "Low-Reynolds-number flow around an oscillating circular cylinder at low Keulegan–Carpenter numbers". *J. Fluid Mech.,* ***360***, pp. 249–271.

[26] Tatsuno, M., and Bearman, P. W., 1990. "A visual study of the flow around an oscillating circular cylinder at low Keulegan-Carpenter numbers and low Stokes numbers". *J. Fluid Mech.,* ***211***, pp. 157–182.

[27] Lamb, H., 1932. *Hydrodynamics*. Cambridge University Press, Dover, NY.

[28] Cimbala, J. M., Nagib, H. M., and Roshko, A., 1988. "Large structure in the far wakes of two-dimensional bluff bodies". *J. Fluid Mech.,* ***190***, pp. 265–298.

[29] Johnson, S. A., Thompson, M. C., and Hourigan, K., 2004. "Predicted low frequency structures in the wake of elliptical cylinders". *Eur. J. Mech. B-Fluid,* ***23***, pp. 229–239.

[30] Leontini, J. S., Stewart, B. E., Thompson, M. C., and Hourigan, K., 2006. "Wake state and energy transitions of an oscillating cylinder at low Reynolds number". *Phys. Fluids,* ***18***(3), p. 067101.

